ISSN (Print) 1226-1750
ISSN (Online) 2233-6656
Journal of Magnetics 26(2), 216-220 (2021) https://doi.org/10.4283/JMAG.2021.26.2.216

Magnetic Properties of Cobalt Substituted Nickel-Zinc Mixed Ferrites

Muhammad Samir Ullah[1]*, Kaniz Fatama[2], Md. Firoz Uddin[1], and Mohammad Mizanur Rahman[2]

[1]*Department of Physics, Bangladesh University of Engineering and Technology, Dhaka-1000, Bangladesh*
[2]*Department of Physics, University of Dhaka, Dhaka-1000, Bangladesh*

(Received 14 August 2020, Received in final form 9 April 2021, Accepted 10 May 2021)

The compositions of Co substituted Ni-Zn ferrites having the formula $Ni_{0.65-x}Co_xZn_{0.35}Fe_2O_4$ (where x = 0.00, 0.01, 0.03, 0.05, 0.07 and 0.09) were prepared by the solid state reaction method and sintered at 1350 °C. The structural property was observed with X-ray diffraction (XRD) method and it showed the single phase cubic spinel structure. Saturation magnetization (M_s), experimental magnetic moment (n_{exp}) and coercive field (H_c) have been investigated. It was observed that the larger value of M_s was found at x = 0.03 due to its stronger super-exchange interaction between two sub-lattices in the spinel ferrites. However, M_s decreases for $0.05 \leq x \leq 0.09$ due to the effect of Yafet-Kittle angle. All the compositions are found to be smaller value of H_c, which indicates the magnetic softness nature of the spinel ferrites. The initial permeabilities were increased which could be attributed to the densification of the samples.

Keywords : ferrite, saturation magnetization, exchange interaction, permeability, compositions

1. Introduction

Ni-Zn mixed ferrites are an useful advanced materials which have a vital role in modern technology such as electromagnetic wave absorbers, inductors, power transformers, phase shifters, antenna rods, memory devices and magnetic recording heads [1, 2]. Cobalt ferrite ($CoFe_2O_4$) is a hard magnetic material having with positive anisotropy constant, incredible mechanical hardness and chemical stability [3]. The magnetic properties of the spinel ferrites are depended on the crystal structure, cation configuration, the type of dopants or substituents, sintering temperature, microstructure and chemical composition [4, 5]. Ferrites are generally prepared by conventional ceramic technology through solid state reactions, which is associated with high sintering temperature and longer annealing time in order to obtain more densification and homogeneity of samples [6]. Ghodake *et al*. studied the initial permeability of Zn-Ni-Co ferrite and they found that the initial permeability (μ_i') was enhanced with a small amount of Co content in Ni-Zn ferrites at the sintering temperature 1150 °C [7]. On the other hand, Hossain *et al*. observed the initial permeability for $Ni_{0.60}Zn_{0.40}Fe_2O_4$ and it was found to be maximum at the optimum sintering temperature 1350 °C [8]. In order to obtain the magnetic softness nature of the materials from the applications point of view, it is required to increase the permeability with smaller coercive field (H_c) in the spinel ferrites. In this regard, the various amount of Co doped Ni-Zn ferrites compositions were performed with complex permeability spectra and magnetic hysteresis experiment along with coercivity of the materials in order to observe the magnetic softness nature of the ferrites. In the present study, $Ni_{0.65-x}Co_xZn_{0.35}Fe_2O_4$ compositions were prepared with solid state reaction method and an attempt has been taken to investigate the structural and magnetic properties of Co substituted Ni-Zn ferrites and explained their results.

2. Experimental

The compositions of ferrites having the formula $Ni_{0.65-x}Co_xZn_{0.35}Fe_2O_4$ (where x = 0.0, 0.01, 0.03, 0.05, 0.07 and 0.09) were synthesized by the solid state reaction method. Appropriate amount of high purity powders of NiO, CoO, ZnO and Fe_2O_3 were used as raw materials. These materials with stoichiometric proportions were weighed and mixed thoroughly with milling for 6 hrs using in ceramic mortar and pestle. Then the mixed powders were pre-sintered at 700 °C for 4 hrs. The calcined powders

*Corresponding author: Tel: +8801782069938
Fax: +880-2-58613046, e-mail: samirullah@phy.buet.ac.bd

were grinded with milling for 2 hrs. The calcined powders were mixed with 1 wt% polyvinyl alcohol (PVA) as a binder and uniaxially pressed to form disk and toroid shaped samples and finally, the prepared samples were sintered at 1350 ºC for 4 hrs in air. An X-ray diffractometer was used to study the crystalline phases of the prepared samples at room temperature in the range from 15º to 70º with Cu-K_α radiation (λ = 1.5424 Å). The surface morphology of the sample was investigated on the polished side surface by Field Emission Scanning Electron Microscopy (JEOL JSM-7600F). The coercive fields were observed with magnetic hysteresis loops using a Vibrating Sample Magnetometer (VSM, EV9, Micro Sense) at room temperature. The variation of the initial magnetic permeability with applied frequency for Co doped Ni-Zn ferrites compositions were measured on toroid shape sample using Wayne-Kerr analyzer (WK 6500B) at room temperature from 20 Hz to 120 MHz.

3. Results and Discussion

Figure 1 shows the X-ray diffraction (XRD) results for the ferrite samples of $Ni_{0.65-x}Co_xZn_{0.35}Fe_2O_4$ sintered at 1350 ºC. The X-ray analysis reveals that the samples are in good crystalline in nature due to its sharp peaks in XRD pattern. The observed peaks are indexed with (111), (220), (311), (222), (400), (422), (511) and (440) planes. These characteristic planes ensured that all the prepared samples were formed the cubic spinel structure [9].

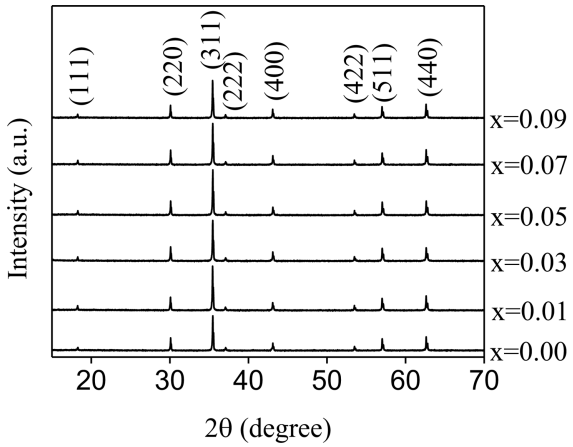

Fig. 1. X-ray diffraction patterns for $Ni_{0.65-x}Co_xZn_{0.35}Fe_2O_4$ compositions.

The FESEM images of $Ni_{0.65-x}Co_xZn_{0.35}Fe_2O_4$ are shown in Fig. 2. The average grain size was calculated with the linear intercept method and it is depicted in Table 1. It can be observed that the relatively larger grain size was obtained at x = 0.07. It is seen from Fig. 3 that the porosity of all samples decreases with increasing of Co contents. The slightly increase in the grain size could be happened due to the higher sintering temperature and the reduction of porosity of the samples [10].

The change in magnetization with applied magnetic

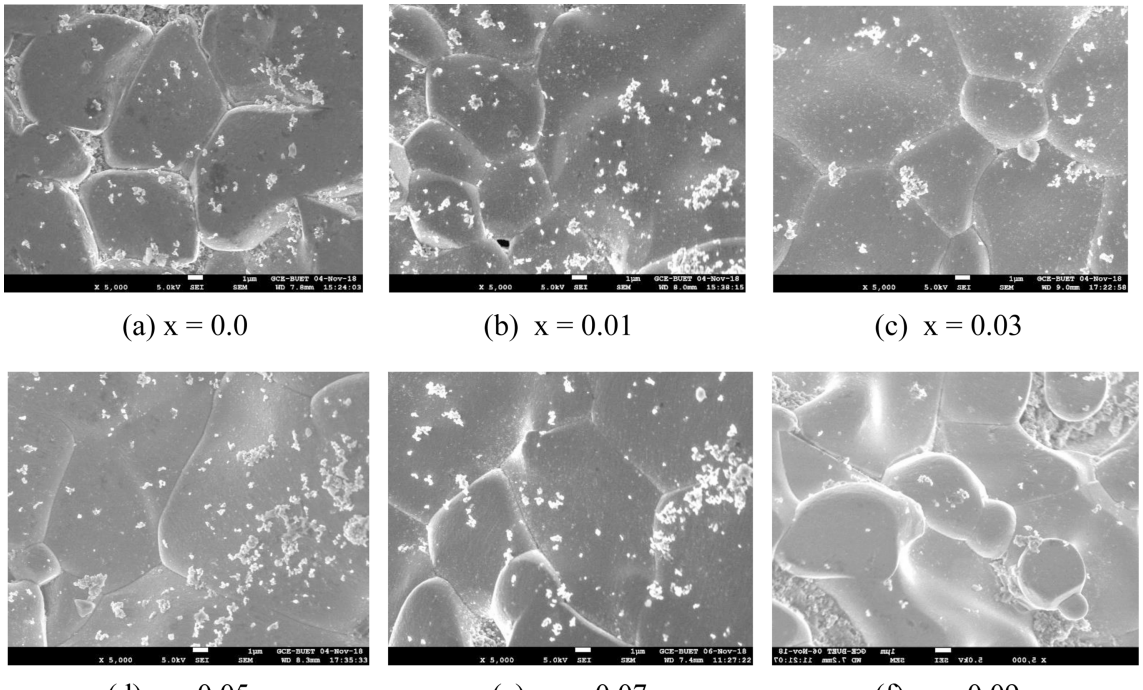

(a) x = 0.0 (b) x = 0.01 (c) x = 0.03

(d) x = 0.05 (e) x = 0.07 (f) x = 0.09

Fig. 2. FESEM photographs for $Ni_{0.65-x}Co_xZn_{0.35}Fe_2O_4$ compositions.

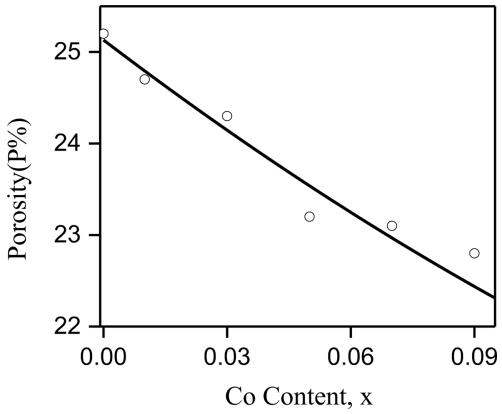

Fig. 3. Variation of porosity (P%) with Co contents, x.

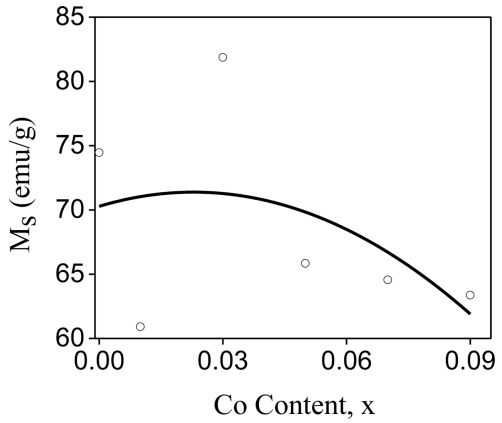

Fig. 4. Variation of saturation magnetization (M_s) with Co contents, x.

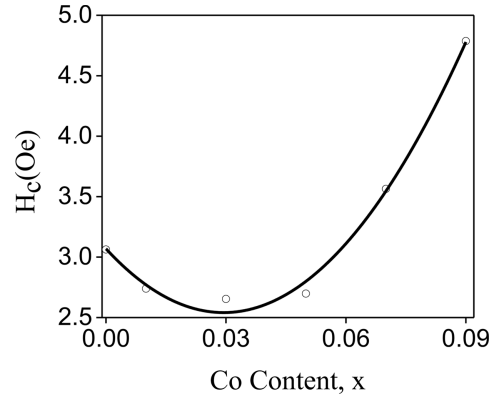

Fig. 5. Variation of Coercive field (H_C) with Co contents, x.

field for $Ni_{0.65-x}Co_xZn_{0.35}Fe_2O_4$ different compositions were performed at room temperature using a Vibrating Sample Magnetometer (VSM). In VSM characterization, the magnetization increases with increasing applied magnetic field and attains its saturation value. It is also observed that all the samples have typical magnetic hysteresis. The variation of saturation magnetization (M_s) with Co content is presented in Fig. 4. The cation distribution of $Ni_{0.65-x}Co_xZn_{0.35}Fe_2O_4$ spinel lattice can be as follows $(Zn^{2+}_{0.35}Fe^{3+}_{0.65})_A\ [Ni^{2+}_{0.65-x}Co^{2+}_{x}Fe^{3+}_{1.35}]_BO^{2-}_4$ where the first term within the first bracket indicates the tetrahedral (A) sites and the second term within the square bracket indicates the octahedral (B) sites. In this distribution formula, Zn^{2+} ions preferred to A sites, whereas Ni^{2+} and Co^{2+} ions are occupied in B sites, but Fe^{3+} ions are distributed in both A and B sites. It is known that the ionic magnetic moments of Zn^{2+}, Ni^{2+}, Co^{2+} and Fe^{3+} are 0, 2, 3 and 5 μ_B, respectively, where μ_B is the Bohr magneton, and the theoretical magnetic moment (n_{th}) is given by

$$\begin{aligned} n_{th} &= \mathcal{M}_B - \mathcal{M}_A \\ &= (8.05 + x)\mu_B - 3.25\,\mu_B \\ &= (4.80 + x)\mu_B \end{aligned} \tag{1}$$

where $\mathcal{M}_A$ and $\mathcal{M}_B$ are the magnetic moment in the A and B sites, respectively. The values of n_{th} with Co content for different values of x are given in Table 1. It can be seen that theoretical magnetic moment increases in linear fashion with increasing of Co contents. The experimental magnetic moment (n_{exp}) in Bohr magneton was calculated by [11]

$$n_{\text{exp}} = \frac{M M_s}{5585} \tag{2}$$

where M is the molecular weight of the sample and M_s is the saturation magnetization. The variation of n_{exp} with Co content for different compositions is also shown in Table 1. Saturation magnetization was found to be maximum at x=0.03 due to the stronger A-B super exchange interactions based on Neel's two sub-lattice collinear models [12]. However, saturation magnetizations were decreased for x > 0.03, which results can be explained on the basis of non-collinear spin structure due

Table 1. Theoretical magnetic moment (n_{th}), Experimental magnetic moment (n_{th}), Y-K angle (θ_{Y-K}), Average grain size (D).

Compositions	n_{th} (μ_B)	n_{exp} (μ_B)	θ_{Y-K} (deg.)	D (μm)
$Ni_{0.65}Zn_{0.35}Fe_2O_4$	4.80	3.20	36.75	6.52
$Ni_{0.64}Co_{0.01}Zn_{0.35}Fe_2O_4$	4.81	2.60	43.46	5.87
$Ni_{0.62}Co_{0.03}Zn_{0.35}Fe_2O_4$	4.83	3.50	33.34	6.06
$Ni_{0.60}Co_{0.05}Zn_{0.35}Fe_2O_4$	4.85	2.80	41.67	6.72
$Ni_{0.58}Co_{0.07}Zn_{0.35}Fe_2O_4$	4.87	2.75	42.38	7.13
$Ni_{0.56}Co_{0.09}Zn_{0.35}Fe_2O_4$	4.89	2.60	44.05	5.52

to the Yafet-Kittle (Y-K) angle effect [13]. The Y-K angle is given by equation [14]

$$n_{exp} = \mathcal{M}_B(x)cos\theta_{Y-K} - \mathcal{M}_A(x) \quad (3)$$

$$cos\theta_{Y-K} = \frac{(n_{exp}+\mathcal{M}_A)}{\mathcal{M}_B} \quad (4)$$

where θ_{Y-K} is the canted angle and given in Table 1. It can be observed that θ_{Y-K} were increased which can be reduced M_s for x > 0.03 due to increase of stronger B-B super exchange interaction from the non-collinear spin structure in the octahedral sites of the spinel lattice. The abrupt changes in saturation magnetization in between x=0.00 to x=0.03 might be the cause of the fluctuation of Y-K angle (θ_{Y-K}) in the spinel sub-lattice. The magnetic parameter, in namely, the coercive field or coercivity (H_c) was determined and is presented in Fig. 5. It can be seen that the coercivity are lowered for 0.01 ≤ x ≤ 0.05 and it increases for 0.07 ≤ x ≤ 0.09, which can be explained based on the Stoner-Wohlfarth [15], the relation between H_c and M_s is

$$H_c = \frac{0.98K}{M_s} \quad (5)$$

where K is the anisotropy constant. The increase in coercivity for 0.07 ≤ x ≤ 0.09 can be suggested from the reduction of the saturation magnetization (M_s) which is consistent with the equation (5). The smaller values (< 75 Oe) of coercivity for all samples are shown the magnetic softness nature of the samples [16].

The complex magnetic permeability measurements on the toroid shape specimens were performed at room temperature for all samples of $Ni_{0.65-x}Co_xZn_{0.35}Fe_2O_4$ in the frequency range 20 Hz-120 MHz. The variation of real part of the initial permeability (μ') and imaginary part

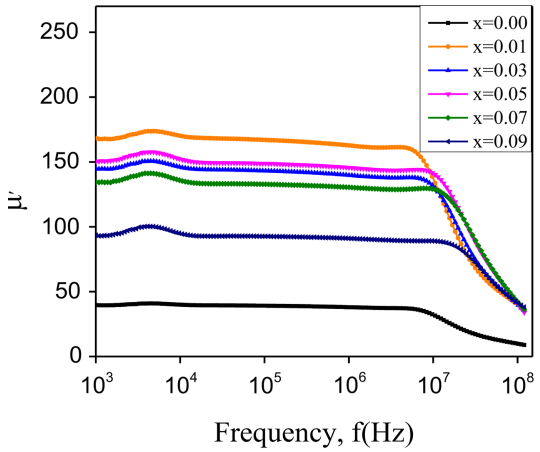

Fig. 6. (Color online) Variation of the real part of the initial permeability with frequency.

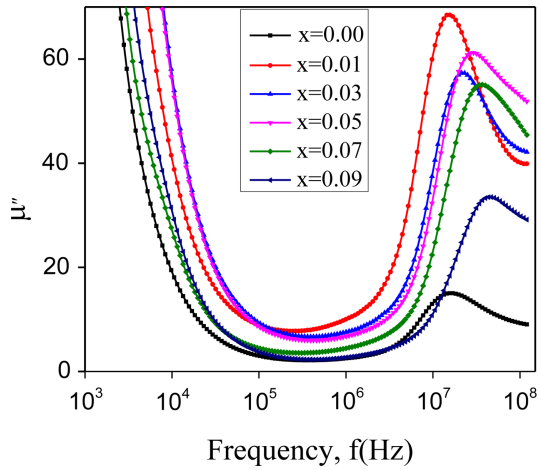

Fig. 7. (Color online) Variation of the imaginary part of the initial permeability with frequency.

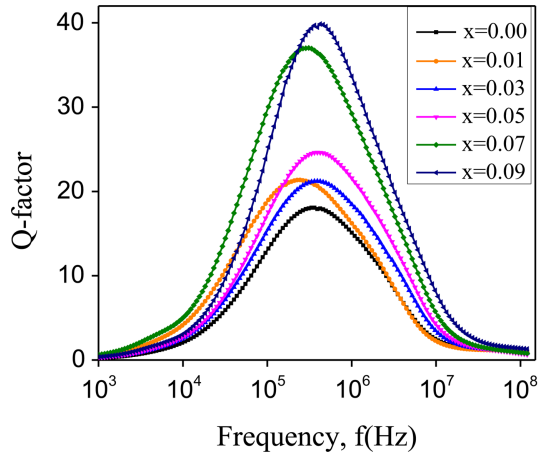

Fig. 8. (Color online) Variation of the Q-factor with frequency.

of the initial permeability (μ'') with applied frequency are shown in Fig. 6 and Fig. 7, respectively. It is observed from Fig. 6 that μ' remains constant in the frequency range up to a certain frequency characterized by the onset of resonance, after a small rise, then curves drop rapidly to a very lower value. On the other hand, it can be seen from Fig. 7 that μ'' rises in gradually and then a broad maximum occurs at a certain frequency, where μ' starts to decrease. This is called ferrimagnetic resonance [17]. It is also observed that the values of the initial permeability (μ_i') are enhanced in Co containing Ni-Zn ferrites. The increase of μ_i' can be attributed to the densification of the samples at higher sintering temperature [18]. The study of Quality factor (Q-factor) is an important property in order to identify the perfect frequency band at which the sample works as soft magnetic material. Fig. 8 shows the variation of the Q-factor with applied frequency for all samples sintered at 1350 °C. It is seen that Q-factor

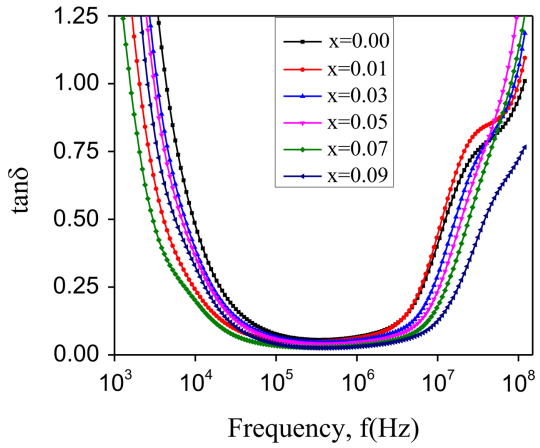

Fig. 9. (Color online) Variation of loss tangent (tan δ) with frequency.

declines beyond 1.0 MHz. The loss tangent is minimum around 1.0 MHz and then it rises rapidly. This is shown in Fig. 9. This loss is associated with the lag of domain wall motion with respect to the applied frequency due to the various defects of domains [14].

4. Conclusions

The ferrites with different compositions $Ni_{0.65-x}Co_x$-$Zn_{0.35}Fe_2O_4$ were synthesized using standard solid state reaction method. All the samples have shown the cubic spinel structure. Saturation magnetization was found to be larger at x = 0.03 composition due to the stronger A-B super exchange interaction, but M_s decreases for x > 0.03 with increasing of Y-K angle due to the non-collinear spin structure in the octahedral sites of the spinel lattice. The smaller value of coercivity is indicated the magnetically soft materials for all samples. These compositions can be used in the magnetic recording devices. The complex permeability spectra measurements shown that the permeability enhancement is reflected from Co substituted Ni-Zn ferrites. It is also observed that Q-factors are enhanced in Ni-Co-Zn ferrites. These findings may be helpful for the electronic and telecommunication industries due to the magnetic devices.

Acknowledgment

The authors are greatly acknowledge to the Department of Physics, Bangladesh University of Engineering & Technology, and Department of GCE, Bangladesh University of Engineering & Technology, and Materials Science Division, Bangladesh Atomic Energy Commission for providing help to carry out of this research work.

References

[1] J. S. Ghodake, R. C. Kambale, T. J. Shinde, P. K. Maskar, and S. S. Suryavanshi, J. Magn. Magn. Mater. **401**, 938 (2016).
[2] X. Huang, J. Zhang, Min Lai, and Tianyi Sang, J. Alloys Compd. **627**, 367 (2015).
[3] K. Zhang, T. Holloway, and A. K. Pradhan, J. Magn. Magn. Mater. **323**, 1616 (2011).
[4] S. M. Hoque, M. S. Ullah, F. A. Khan, M. A. Hakim, and D. K. Saha, Physica B **406**, 1799 (2011).
[5] I. Soibam, S. Phanjoubam, and C. Prakash, J. Magn. Magn. Mater. **321**, 2779 (2009).
[6] K. Raju, G. Venkataiah, and D. H. Yoon, Ceram. Int. **40**, 9337 (2014).
[7] J. S. Ghodak, T. J. Shinde, R. P. Patil, S. B. Patil, and S. S. Surayavanshi, J. Magn. Magn. Mater. **378**, 436 (2015).
[8] A. K. M. A. Hossain, S. T. Mahmud, M. Seki, T. Kawai, and H. Tabata, J. Magn. Magn. Mater. **312**, 210 (2007).
[9] B. D. Cullity, Elements of X-ray Diffraction. Addison Wesley Publishing Company, Inc., Massachusetts, USA.
[10] Sea-Fue Wang. Yung-Fu Hsu, Kai-Mou Chou, and Jeng-Ting Tsai, J. Magn. Magn. Mater. **374**, 402 (2015).
[11] T. J. Shinde, A. B. Gadkari, and P. N. Vasambekar, J. Magn. Magn Mater. **333**, 152 (2013).
[12] J. Smith and H. P. J. Wijn, Ferrites, Wiley, New York (1959).
[13] T. T. Ahmed, I. Z. Rahman, and M. A. Rahman, J. Mat. Pro. Tech. **153-154**, 797 (2004).
[14] M. M. Haque, M. Huq, and M. A. Hakim, Physica B **404**, 3915 (2009).
[15] G. Gan, D. Zhang, Q. Zhang, G. Wang, X. Huang, Y. Yang, Y. Rao, Jei Li, Fang Xu, X. Wang, R. T. Chen, and H. Zhang, Ceram. Int. **45**, 12035 (2019).
[16] J. Du, G. Yao, Y. Liu, J. Ma, and G. Zu, Ceram. Int. **38**, 1707 (2012).
[17] Y. P. Fu and S. H. Hu, Ceram. Int. **36**, 1311 (2010).
[18] S. M. Hoque, M. A. Choudhury, and M. F. Islam, J. Magn. Magn. Mater. **251**, 292 (2002).